Autonomous Light Control by Wireless Sensor and Actuator Networks

Lun-Wu Yeh, Che-Yen Lu, Chi-Wai Kou, Yu-Chee Tseng, *Senior Member, IEEE*, and Chih-Wei Yi, *Member, IEEE*

***Abstract*—Recently, wireless sensor and actuator networks (WSANs) have been widely discussed in many applications. In this paper, we propose an autonomous light control system based on the feedback from light sensors carried by users. Our design focuses on meeting users' preferences and energy efficiency. Both whole and local lighting devices are considered. Users' preferences may depend on their activities and profiles and two requirement models are considered: binary satisfaction and continuous satisfaction models. For controlling whole lighting devices, two decision algorithms are proposed. For controlling local lighting devices, a surface-tracking scheme is proposed. Our solutions are autonomous because, as opposed to existing solutions, they can dynamically adapt to environment changes and do not need to track users' current locations. Simulations and prototyping results are presented to verify the effectiveness of our designs.**

***Index Terms*—Intelligent building, LED, light control, pervasive computing, wireless communication, wireless sensor and actuator network.**

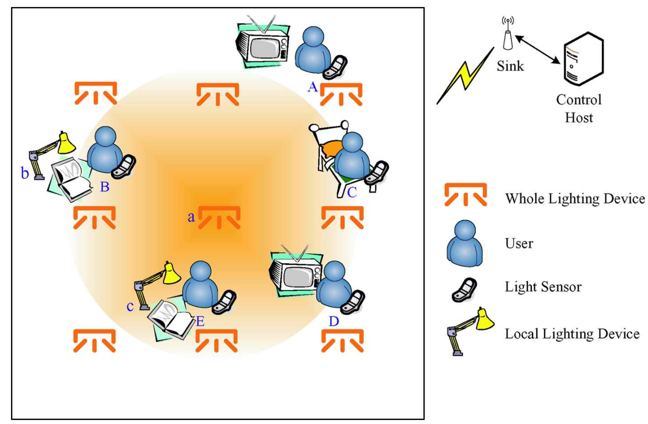

Fig. 1. The network scenario of our system.

I. Introduction

THE rapid progress of wireless communications and embedded MEMS technologies has made *wireless sensor and actuator networks* (WSANs) possible. A WSAN [1]–[3] is a distributed system consisting of sensor and actuator nodes interconnected by wireless links. Using sensed data from sensor nodes, actuators can perform actions accordingly. The possible applications of WSANs include smart living space [4], localization [5], [6], environmental monitoring [7], [8], etc.

Recently, WSANs have been applied to energy conservation applications such as light control [9]–[12]. The decision of lighting control can be made based on the daylight intensity sensed by light sensors [12]. In [10], the authors defined several user requirements and cost functions. Their goal was to adjust lights to minimize the total cost. However, the result was applied to entertainment and media production systems. In [11], a tradeoff between energy consumption and user's satisfaction in light control was studied. The authors applied the utility functions which consider users' location and lighting preferences to adjust illuminations so as to maximize the total utilities. However, it did not consider the fact that people need different illuminations under different activities. The heuristics proposed in [10] and [11] need to measure all combinations of dimmer settings and the resulting illuminations at all locations, so if there are k interested locations, d dimmer levels, and m lighting devices, the measurement complexity is $O(kdm)$. In [9], for pervasive sensors deployment, the measuring time complexity was further reduced to $O(km)$. The goal was to satisfy users' demands while optimizing energy efficiency. These works all relied on knowing users' current locations, so extra localization mechanisms were needed.

In this work, we propose a light control system that considers both users' preferences and energy conservation. Fig. 1 shows a typical network scenario in which users carry light sensors and lighting devices are controllable. Sensors can help each other to relay sensing data to the sink node. Then, the control host can give commands to lighting devices based on collected data. Here, we consider LED lighting devices [13], [14] and they are categorized into *whole* and *local lighting devices*. The former can provide background illuminations for multiple users in wide areas, and the latter is similar to desk lamps that provide concentrated illuminations. For example, in Fig. 1, device a in the center can provide background illuminations for user B, C and E, and device b can only provide concentrated illumination for user B.

In our system, users may have different illumination requirements according to their activities and profiles. Two types of requirements, *background* and *concentrated* ones, are considered. For example, in Fig. 1, user A is watching television, B is reading a book, and C is sleeping. Both A and B require the same background illuminations, but B needs concentrated illumination. C does not require neither background nor concentrated illuminations. A user is said to be *satisfied* if the provided background and concentrated illuminations fall into the required ranges. To evaluate the satisfaction level of a user, we

Manuscript received October 04, 2009; revised January 13, 2010; accepted January 17, 2010. Current version published April 02, 2010. The associate editor coordinating the review of this paper and approving it for publication was Prof. Evgeny Katz.

The authors are with the Department of Computer Science, National Chiao-Tung University, Hsin-Chu City 30010, Taiwan (e-mail: lwyeh@cs.nctu.edu.tw; chaos@cs.nctu.edu.tw; kaocw@cs.nctu.edu.tw; yctseng@cs.nctu.edu.tw; yi@cs.nctu.edu.tw).

Color versions of one or more of the figures in this paper are available online at http://ieeexplore.ieee.org.

Digital Object Identifier 10.1109/JSEN.2010.2042442

further consider a *binary satisfaction model* and a *continuous satisfaction model*. The former only returns a satisfaction value of 1 or 0, while the latter returns a value between 0 and 1. We develop two algorithms to adjust whole lighting devices for these models with the goals of meeting users' requirements while minimizing energy consumption. In case that it is impossible to satisfy all users simultaneously, we will gradually relax users' requirements until all users are satisfied. For concentrated illuminations, assuming that local lighting devices are moveable (which can be supported by robot arms), we develop a novel "surface-tracking" scheme to track local movements of users to provide required illuminations.

The main contributions of this work are twofold. First, our model is designed for "point-like" light sources, such as LEDs, which are more energy-efficient than traditional light sources and are expected to be the mainstream of lighting technologies in the future. We show how to take advantage of its light propagation property to conduct light control. Second, compared to existing solutions, our solution is "autonomous" in the sense that it can dynamically adapt to environment changes and does not need extra scheme to track users' locations. Hence, our work relaxes the requirement of an underlying localization mechanism in existing works.

The rest of this work is organized as follows. Section II presents the system model. Sections III and IV introduce our control algorithms for background and concentrated light sources, respectively. Section V contains simulation results. Section VI presents our prototyping results. Conclusions are drawn in Section VII.

II. System Model

A. Light Measurement Method

In our system, there are n users, $u_1, u_2, \ldots, u_n$, m whole lighting devices, $D_1, D_2, \ldots, D_m$, and m' local lighting devices, $d_1, d_2, \ldots, d_{m'}$. The lighting devices are controllable. For all $i = 1, 2, \ldots, n$, user u_i carries a light sensor s_i which periodically reports an illumination level P_i sensed by the sensor to the control host. The luminous intensity emitted by D_j is denoted by C_j^D, and that by d_j is denoted by C_j^d. Considering physical limitations, we assume that C_j^D and C_j^d should satisfy $C_j^{D_{\min}} \leq C_j^D \leq C_j^{D_{\max}}$ and $C_j^{d_{\min}} \leq C_j^d \leq C_j^{d_{\max}}$.

We make the following assumptions in our work. First, there exists a natural light source, but it may change over time. Second, artificial light sources are assumed to be "point-like" ones such as LEDs. This makes modeling the impact of light sources easier. For whole lighting sources, disturbance from other objects may exist (such as furniture, obstacles, walls, etc.). However, we assume that it is possible to derive the impact of a whole lighting device on a sensor. That allows us to decide the proper intensity of each light source. For local lighting sources, we assume that no such disturbance exists. So, we can derive the distance between a lighting source and a user based on the measurement of light sensors. In addition, we assume that local lighting sources are mounted on robot arms and thus the position and orientation of local lighting sources are controllable. We will discuss more about this in Section IV.

Next, we explain how to model the impact of a light source X_j on a light sensor s_i. Here, X_j can be a whole lighting source D_j or a local lighting source d_j (See Fig. 2). Let l and h be the distances from X_j to s_i and to the nearest ground, respectively. Now let X_j increase its intensity by ΔC_j^X candela, and we measure the change of illumination $\Delta L_{i,j}$ at s_i. According to the light propagation property, we have

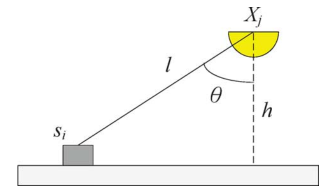

Fig. 2. Measuring the impact of a light source X_j on a light sensor s_i.

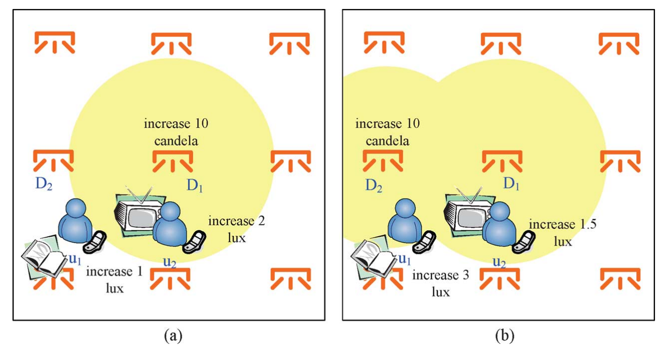

Fig. 3. An example of weight measurement.

$$\Delta L_{i,j} = \frac{\Delta C_j^X \times \cos\theta}{l^2} = \frac{\Delta C_j^X \times h}{l^3}. \tag{1}$$

From ΔC_j^X and the observed $\Delta L_{i,j}$, we define the impact of X_j on s_i as

$$w_{i,j}^X = \frac{\Delta L_{i,j}}{\Delta C_j^X} = \frac{h}{l^3}. \tag{2}$$

Intuitively, this implies that even if l and h are unknown, we can still measure the weight $w_{i,j}^X$ from ΔC_j^X and $\Delta L_{i,j}$. Therefore, we can easily decide the amount of increment/decrement on X_j's intensity to achieve the desired level of illumination sensed by s_i. Below, if $X_j = D_j$, the impact is written as $w_{i,j}^D$; if $X_j = d_j$, it is written as $w_{i,j}^d$. The measurement of impact values should be done one-by-one, so the overall time complexity is $O(m + m')$. In comparison, this is much lower than those in [9], [10] and [11]. Besides, in our work, we can further consider measuring the impacts of some lighting devices and using interpolation techniques to estimate the impacts of remaining lighting devices to further reduce the measurement cost.

The key technique to the above weight measurement is to slightly increase each light source's intensity one-by-one. In the example illustrated in Fig. 3(a), if D_1 increases 10 candela and the light intensities sensed by u_1 and u_2 increase by 1 and 2 lux, respectively, then we can get $w_{1,1}^D = 1/10 = 0.1$ and $w_{2,1}^D = 2/10 = 0.2$. Similarly, in Fig. 3(b), if D_2 increases 10 candela and the light intensities sensed by u_1 and u_2 increase by 3 and 1.5 lux, then we can get $w_{1,2}^D = 3/10 = 0.3$ and $w_{2,2}^D = 1.5/10 = 0.15$.

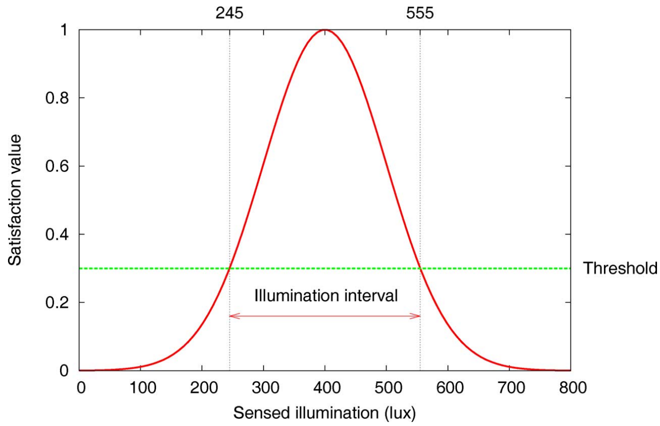

Fig. 4. An example of continuous satisfaction.

Because illuminations are additive [11], the light intensity sensed by s_i, denoted as P_i, is the sum of the natural light L_i^{na} and the illuminations provided by the whole and local lighting devices, i.e.,

$$P_i \approx \sum_{j=1}^{m} (w_{i,j}^D \times C_j^D) + \sum_{j=1}^{m'} (w_{i,j}^d \times C_j^d) + L_i^{na}. \quad (3)$$

P_i is called the concentrated illumination perceived by u_i, and the background illumination perceived by u_i is estimated by $P_i - \sum_{j=1}^{m'} (w_{i,j}^d \times C_j^d)$. In this work, we consider two kinds of user satisfaction models for illuminations:

1) *Binary satisfaction model*: Each user u_i has an acceptable background illumination interval $[R_i^{bl}, R_i^{bu}]$ and an acceptable concentrated illumination interval $[R_i^{cl}, R_i^{cu}]$. The user is said to be *satisfied* if its concentrated and background illuminations fall within these intervals, respectively.
2) *Continuous satisfaction model*: Each user u_i has concentrated and background illumination requirements, but they are specified by utility-like functions.[1] The satisfaction value is given by a normal-distribution-like function with parameter μ_i, σ_i, and t_i. If x denotes the illumination, the satisfaction value $f_i(x)$ is defined as given in (4) at the bottom of the page. For the background illumination (or the concentrated illumination, respectively), we denote the three parameters as μ_i^b, σ_i^b and t_i^b (or μ_i^c, σ_i^c and t_i^c, respectively). Fig. 4 shows an example of continuous model with $\mu = 400$, $\sigma = 100$, and $t = 0.3$.

Note that for concentrated illuminations, we assume that it is always possible to meet users' requirements since local lighting devices are very close to users, so no particular model is specified.

[1]The work [11] adopts a curve function to represent users' lighting preferences. In this work, we adopt Gaussian functions to represent users' lighting preferences. However, it is not hard to extend to other utility functions.

B. Control Flow

Fig. 5 illustrates the light control flow of our system. The control process is triggered by user movement, periodical checking, or inputs from sensors which reveal that some users are not satisfied. Then, the weight measurement block determines $w_{i,j}^D$ and $w_{i,j}^d$ that had been discussed in Section II-A. After that, the whole light control and local light control modules follow. The background illumination constraints are achieved by tuning C_j^D for all users based on $\sum_{j=1}^{m} (w_{i,j}^D \times C_j^D) + L_i^{na}$, and the concentrate illumination constraints are achieved by tuning C_j^d for each user based on $\sum_{j=1}^{m} (w_{i,j}^D \times C_j^D) + \sum_{j=1}^{m'} (w_{i,j}^d \times C_j^d) + L_i^{na}$. It turns out that decisions of the whole or local light control can be made independently of each other.

III. Control of Whole Lighting Devices

In this section, we design two solutions for the binary and the continuous satisfaction models. For the binary satisfaction model, the primary goal is to meet all users' requirements. Once the primary goal is met, the secondary goal is to minimize the total energy cost. It is possible that there exists no solution to meet all users' requirements. In such a case, we can compromise by enlarging users' acceptable intervals until all users are satisfied. The details of this issue will be discussed later. After the relaxation, we go to achieve the secondary goal, just like before. For the continuous satisfaction model, since users' satisfaction values are represented by utility functions, there are not too many chances to further optimize the total energy cost. So, in this case, we only adjust light intensities to maximize the total satisfaction value of all users.

A. Binary Satisfaction Model

Our goal is to determine C_j^D for device D_j to meet users' background illumination requirements. Under the binary satisfaction model, we are given the inputs including $w_{i,j}^D$ for all $i = 1, \ldots, n$ and $j = 1, \ldots, m$; L_i^{na}, R_i^{bl} and R_i^{bu} for all $i = 1, \ldots, n$; $C_j^{D_{\min}}$ and $C_j^{D_{\max}}$ for all $j = 1, \ldots, m$. Our goal is to solve C_j^D for all $j = 1, \ldots, m$ with the objective function

$$\min \sum_{j=1}^{m} C_j^D \quad (5)$$

subject to

$$R_i^{bl} \le \sum_{j=1}^{m} (w_{i,j}^D \times C_j^D) + L_i^{na} \le R_i^{bu} \quad \text{for all } i = 1, \ldots, n \quad (6)$$

$$C_j^{D_{\min}} \le C_j^D \le C_j^{D_{\max}} \quad \text{for all} \quad j = 1, \ldots, m. \quad (7)$$

Note that in (6), the $w_{i,j}^D$ can be known by the weight measurement method in Section II-A. In some cases, the initial value of C_j^D is not zero. Hence, we can subtract the initial value to

$$f_i(x) = \begin{cases} \exp\left(\frac{-(x-\mu_i)^2}{2(\sigma_i)^2}\right), & \text{if } x \in [\mu_i - \sigma_i\sqrt{-2\ln(t_i^c)}, \mu_i + \sigma_i\sqrt{-2\ln(t_i^c)}] \\ 0, & \text{otherwise} \end{cases} \quad (4)$$

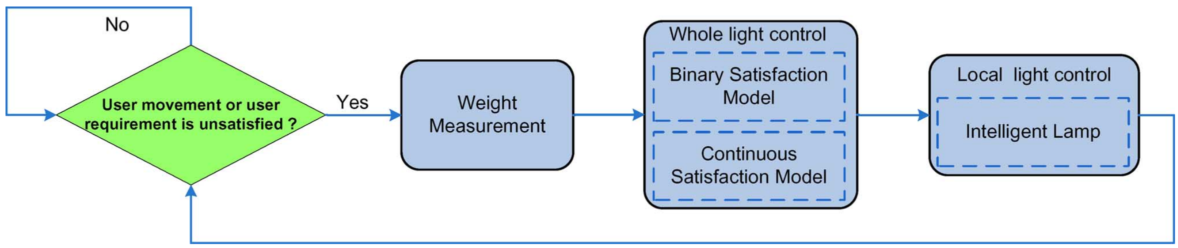

Fig. 5. Light control flow chart.

get the adjustment value for each lighting device. Equation (5) is to minimize the total power consumption of whole lighting devices. Equation (6) imposes that all users' background illumination requirements should be met. Equation (7) is to confine the adjustment result within the maximum and the minimum bounds. Note that $C_j^{D_{\min}} \geq 0$ for all j. This is a linear programming problem and can be solved by, e.g., the Simplex method [15]. Intuitively, the primary goal is to meet all users' requirements. The secondary is to achieve (5). However, in reality, the system may be infeasible. One may try to eliminate the least number of requirements to find a feasible subsolution. However, it was shown that finding a feasible subsystem of a linear system by eliminating the fewest constraints is NP-hard [16]. So, we compromise by gradually relaxing users' requirements to make this problem feasible. Therefore, we propose an iterative process as follows. First, we run the Simplex method. If no feasible solution is found, we change u_i's requirement to $[\max(0, R_i^{bl} - \alpha), R_i^{bu} + \alpha]$ for each $i = 1, \ldots, n$, where α is a constant. Then, we run the Simplex method again. This is repeated until a solution is found. Once all users' requirements are met, we go to minimize the total energy cost.

B. Continuous Satisfaction Model

Under the continuous satisfaction model, the inputs include $w_{i,j}^D$ for all $i = 1, \ldots, n$ and $j = 1, \ldots, m$; $C_j^{D_{\min}}$ and $D_j^{D_{\max}}$ for all $j = 1, \ldots, m$; $(\mu_i^b, \sigma_i^b, t_i^b)$ and L_i^{na} for all $i = 1, \ldots, n$. The goal is to find C_j^D for all $j = 1, \ldots, m$ with the objective function

$$\max \quad \sum_{i=1}^{n} f_i^b \left(\sum_{j=1}^{m} (w_{i,j}^D \times C_j^D) + L_i^{na} \right) \tag{8}$$

subject to

$$\begin{aligned} &\mu_i^b - \sigma_i^b \sqrt{-2\ln(t_i^b)} \\ &\quad \leq \sum_{j=1}^{m} (w_{i,j}^D \times C_j^D) + L_i^{na} \leq \mu_i^b + \sigma_i^b \sqrt{-2\ln(t_i^b)} \\ &\quad \text{for all} \quad (i = 1, \ldots, n) \qquad (9) \\ &C_j^{D_{\min}} \leq C_j^D \leq C_j^{D_{\max}} \quad \text{for all} \quad j = 1, \ldots, m. \qquad (10) \end{aligned}$$

Equation (8) is to maximize the sum of satisfaction values of all users. Equation (9) imposes that all users' background illumination requirements should be met. Equation (10) specifies the bounds. This is a nonlinear programming problem and can be solved by a sequential quadratic programming (SQP) method [17]. If there is no feasible solution, we gradually relax users' requirements to make this problem feasible. We propose an iterative process as follows: First, we run the SQP method. If no feasible solution is found, we change u_i's background threshold to $\max(0, t_i^b - \beta)$ for each $i = 1, \ldots, n$, where β is a constant. Then, we run the SQP method again. This is repeated until a solution is found.

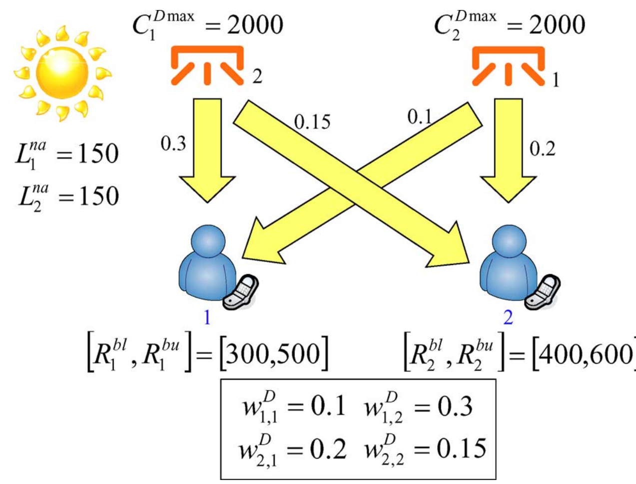

Fig. 6. An example for the binary satisfaction model.

C. Examples

An example of the binary satisfactory model is illustrated in Fig. 6, where there are two users u_1 and u_2, and two whole lighting devices D_1 and D_2. We have $L_1^{na} = 150$, $L_2^{na} = 150$, $[R_1^{bl}, R_1^{bu}] = [300, 500]$, and $[R_2^{bl}, R_2^{bu}] = [400, 600]$. The objective function is

$$\min \quad C_1^D + C_2^D$$

subject to

$$\begin{aligned} &300 \leq 150 + 0.1 \times C_1^D + 0.3 \times C_2^D \leq 500 \\ &400 \leq 150 + 0.2 \times C_1^D + 0.15 \times C_2^D \leq 600 \\ &\quad 0 \leq C_1^D \leq 2000 \\ &\quad 0 \leq C_2^D \leq 2000. \end{aligned}$$

Since this problem is feasible, the solution is $C_1^D = 1166.67$ and $C_2^D = 111.11$. If the current light intensities are $C_1^D = 100$ and $C_2^D = 100$, we need to set $\Delta C_1^D = 1166.67 - 100 = 1066.67$ and $\Delta C_2^D = 111.11 - 100 = 11.11$.

Fig. 7 illustrates an example of the continuous satisfaction model. Similarly, there are two users and two lighting devices. The natural lights are $L_1^{na} = 150$ and

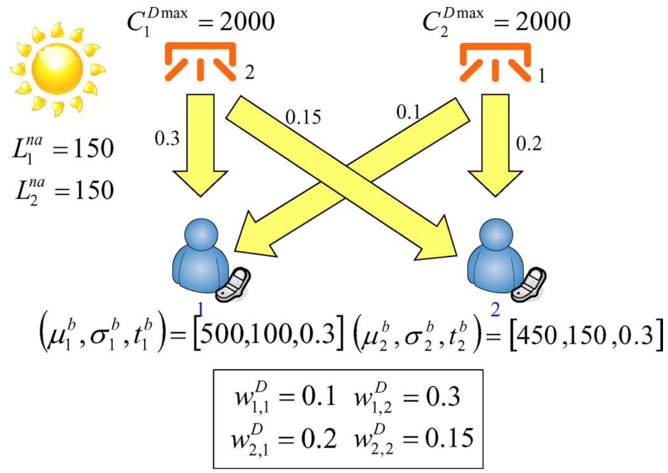

Fig. 7. An example for the continuous satisfaction model.

$L_2^{na} = 150$. We assume that $(\mu_1^b, \sigma_1^b, t_1^b) = (500, 100, 0.3)$ and $(\mu_2^b, \sigma_2^b, t_2^b) = (450, 150, 0.3)$ for u_1 and u_2, respectively. Given $t_1^b = 0.3$ and $t_2^b = 0.3$, we can derive $[\mu_1^b - \sigma_1^b\sqrt{-2\ln(t_1^b)}, \mu_1^b + \sigma_1^b\sqrt{-2\ln(t_1^b)}] = [345, 655]$ and $[\mu_2^b - \sigma_2^b\sqrt{-2\ln(t_2^b)}, \mu_2^b + \sigma_2^b\sqrt{-2\ln(t_2^b)}] = [167, 633]$ for u_1 and u_2, respectively. The objective function is

$$\max \quad f_1^b(150 + 0.1 \times C_1^D + 0.3 \times C_2^D) + f_2^b(150 + 0.2 \times C_1^D + 0.15 \times C_2^D)$$

subject to

$$345 \le 150 + 0.1 \times C_1^D + 0.3 \times C_1^D \le 655$$
$$167 \le 150 + 0.2 \times C_2^D + 0.15 \times C_2^D \le 633$$
$$0 \le C_1^D \le 2000$$
$$0 \le C_2^D \le 2000.$$

Again, this problem is also feasible. The solution is $C_1^D = 355.4$ and $C_2^D = 1066.3$. If the current light intensities are $C_1^D = 100$ and $C_2^D = 100$, we need to set $\Delta C_1^D = 355.4 - 100 = 255.4$ and $\Delta C_2^D = 1066.3 - 100 = 966.3$.

IV. Control of Local Lighting Devices

The above lighting control heuristic algorithms are able to adjust background illuminations to meet users' needs. Here, we are further going to propose a robotic device, called *Intelligent Lamp* (iLamp), to provide concentrated illuminations. An iLamp has a robot arm with at least four local lighting devices and is supposed to serve one user who has need of concentrated illumination. The service scenario is shown in Fig. 8. The sensor should be placed on the reading surface. On detecting a user under its service area, the iLamp will compute its relative location to the light sensor, move via its robot arm to a better location, and then adjust its luminous intensities to meet the need with the least energy. Detecting a nearby user is a simple job since a local lighting device can check if it has non-negative impact on a sensor.

Given an iLamp and a light sensor s_i, they will cooperate with each other by the following four steps to achieve our goal: 1) collect the current P_i sensed by s_i; 2) calculate the location of s_i; 3) adjust the lamp's robot arm; and (4) adjust the luminous intensities of its lighting devices. Step 1 is executed periodically. Once it finds that the current illumination falls outside the required interval, steps 2, 3, and 4 are triggered. Central to our scheme is step 2, so we will elaborate it in more details below.

To drive step 2, assume for simplicity that the iLamp has four local lighting devices d_1, d_2, d_3, and d_4 as shown in the geometry model in Fig. 9(a). Note that it is not hard to extend this result to more lighting devices in other geometry models. Since there is a robot arm, the iLamp should know the coordinate (x_j, y_j, z_j) of d_j, $j = 1, \ldots, 4$. Without loss of generality, regard the projection of d_1 on the reading surface as the origin

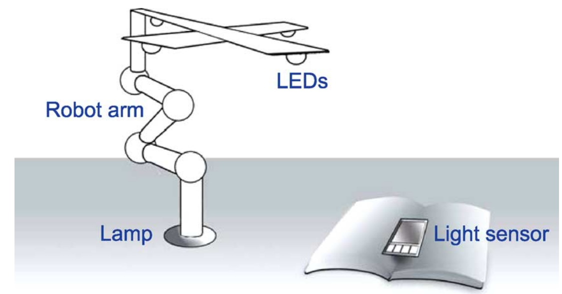

Fig. 8. Service scenario of an iLamp and a light sensor.

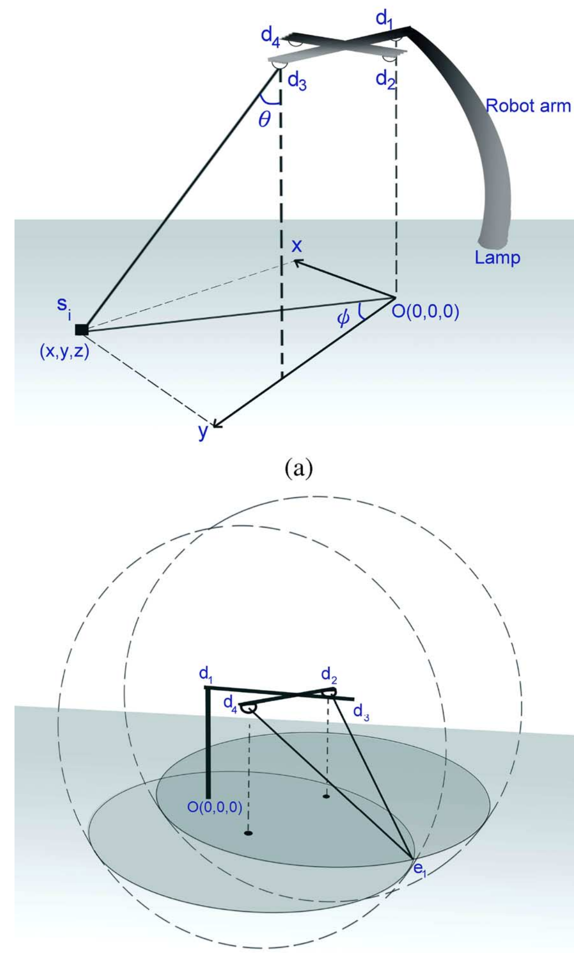

(a)

(b)

Fig. 9. The geometry model of iLamp to track the location of s_i.

$O(0,0,0)$, the projection of $\overrightarrow{d_1 d_3}$ on the surface as the y axis, the projection of $\overrightarrow{d_2 d_4}$ on the surface parallel with the x axis, and the norm of the surface toward the sky as the z axis. Let the location of s_i be $(x, y, z=0)$. We will derive a scheme to find its location as follows. Since LED is a point-like light source, it dissipates identically in all directions. Our scheme consists of two symmetric processes. The first one is to use d_2 and d_4 to estimate two potential locations of s_i, and then use d_1 and d_3 to screen out one location. The second one is to use d_1 and d_3 to estimate two potential locations of s_i, and use d_2 and d_4 to screen out one location. Finally, we take their middle point as the estimated location of s_i.

1) For each $d_j, j=1,\ldots,4$, increase its luminous intensity by ΔC_j candela and measure the change of illuminance intensity at s_i, denote by ΔL_{ij}. According to the definition of illumination, we have the equality

$$\Delta L_{ij} = \frac{\Delta C_j \times \cos\theta_{ij}}{\left(\sqrt{(x-x_j)^2+(y-y_j)^2+(z-z_j)^2}\right)^2}$$

where

$$\cos\theta_{ij} = \frac{z_j}{\sqrt{(x-x_j)^2+(y-y_j)^2+(z-z_j)^2}}.$$

This leads to

$$\Delta L_{ij} = \frac{\Delta C_j \times z_j}{\left(\sqrt{(x-x_j)^2+(y-y_j)^2+(z-z_j)^2}\right)^3}. \quad (11)$$

2) Observe that the equations of ΔL_{i2} and ΔL_{i4} represent two balls centered at d_2 and d_4, respectively. Since it is known that $z=0$, each of these two balls intersects with plane $z=0$ at a circle. These two circles will intersect at two points. Using any equation of ΔL_{i1} and ΔL_{i3}, we can pick one point as the estimated location of s_i, called e_1. [Refer to Fig. 9(b).]
3) Similarly, the equations of ΔL_{i1} and ΔL_{i3} represent two balls at d_1 and d_3, respectively, each intersecting with plane $z=0$ at a circle. Again, these two circles intersect at two points, and we can pick one point as the location of s_i, called e_2, with the assistance of ΔL_{i2} and ΔL_{i4}.
4) Finally, the location of s_i is predicted as the middle point of e_1 and e_2.

In step 3, we move our lighting devices toward the upper side of s_i. This includes two substeps. First, we rotate the robot arm by ϕ angle such that the vector from d_1 to d_3, after projecting to the reading surface, is pointing toward the location of s_i. Second, it moves to the upper side of s_i to provide a proper reading angle (a typical angle is 60°).

Step 4 is to adjust $C_j^d, j=1,\ldots,4$ to meet the concentrated illumination demand of u_i. From the results in Section III, some background and natural illuminations have already been provided. So we only need to add some more light to meet u_i's need. The results in Section III can be directly applied again here, so we omit the details.

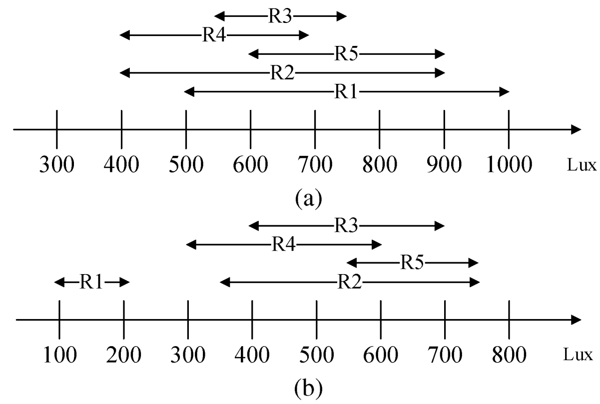

Fig. 10. Requirement pools: (a) $RP1$ and (b) $RP2$.

V. Simulation Results

To understand how our schemes for whole lighting control meet users' requirements while saving energy, we have developed a simulation. Two scenarios are considered. One scenario, denoted as $S1$, is in a room of size $10 \times 10\ \mathrm{m}^2$ with an array of 5 × 5 whole lighting devices. The other scenario, denoted as $S2$, is in a room of size 20 × 20 m^2 with an array of 9 × 9 while lighting devices. We set $C_i^{D_{\min}} = 0$ and $C_i^{D_{\max}} = 3000$ for all i. Our proposed algorithms are compared to other two schemes, called FIX and GREEDY. The FIX scheme is a very intuitive one assuming that users' locations are known in advance. The nearest devices are selected and set to a fixed candela value n. We denote this scheme as FIX-n below. The GREEDY scheme also assumes that users' locations are known. For each user, the nearest device is selected to satisfy the user (if possible). If it is still below the required illumination, the second nearest device is picked to increase the intensity. This is repeated until the user is satisfied. Note that it may happen that a user is satisfied first but later on becomes unsatisfied due to other devices change their intensities. Below, we compare the outcomes according the two satisfaction models introduced in Section II.

- Binary satisfaction model: A requirement pool is a set of requirements. In the simulation, each user will randomly choose one from the pool as its requirement. Two requirement pools, denoted by $RP1$ and $RP2$, are considered. See Fig. 10 in which each range R_i represents an expected illumination interval. We consider two performance indices here. The first index is the total energy consumption. The second index is called GAP, which reflects the difference between the provided illumination and the required one. The GAP for user u_i is

$$\mathrm{GAP}(u_i) = \begin{cases} 0, & \text{if } R_i^{bl} \le P_i \le R_i^{bu} \\ \min(|R_i^{bl} - P_i|, |R_i^{bu} - P_i|), & \text{otherwise.} \end{cases} \quad (12)$$

We will measure the average GAP of all users.

Fig. 11 shows our simulation results under different combinations of $S1/S2$ and $RP1/RP2$. In Fig. 11(a), we see that our scheme is the most energy-efficient while keeping the average GAP close to zero. This is because the requirement intervals in $RP1$ have common overlapping and that allows our system to satisfy all users in most cases. Note that although FIX-1000 uses less energy, its GAP is

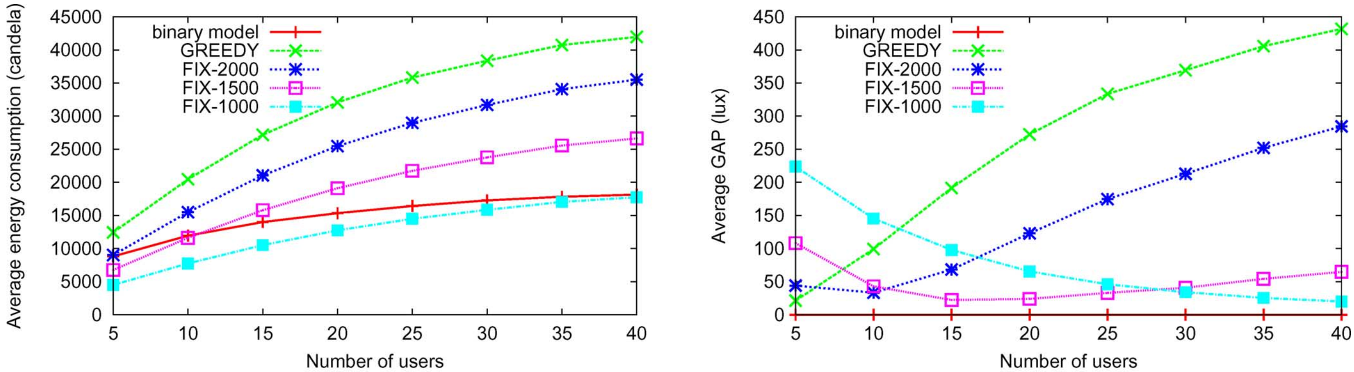

(a)

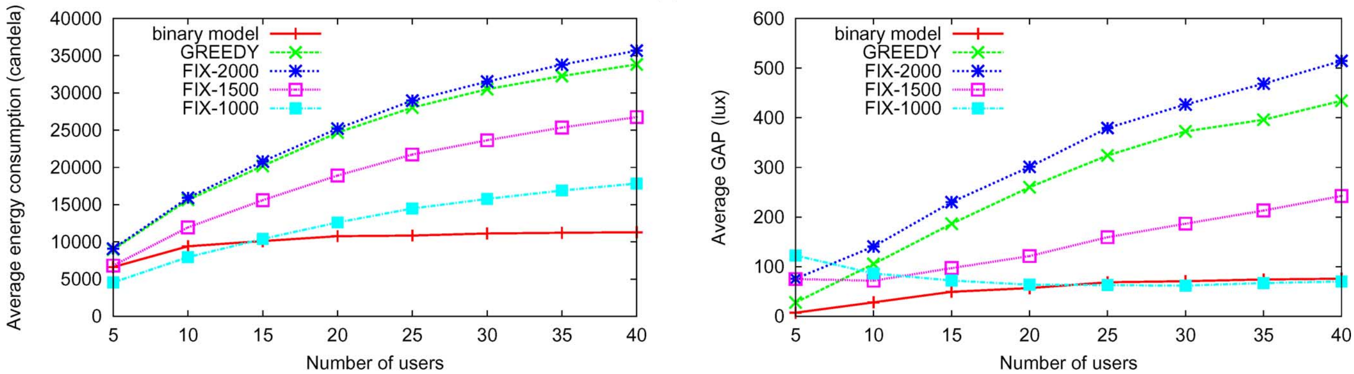

(b)

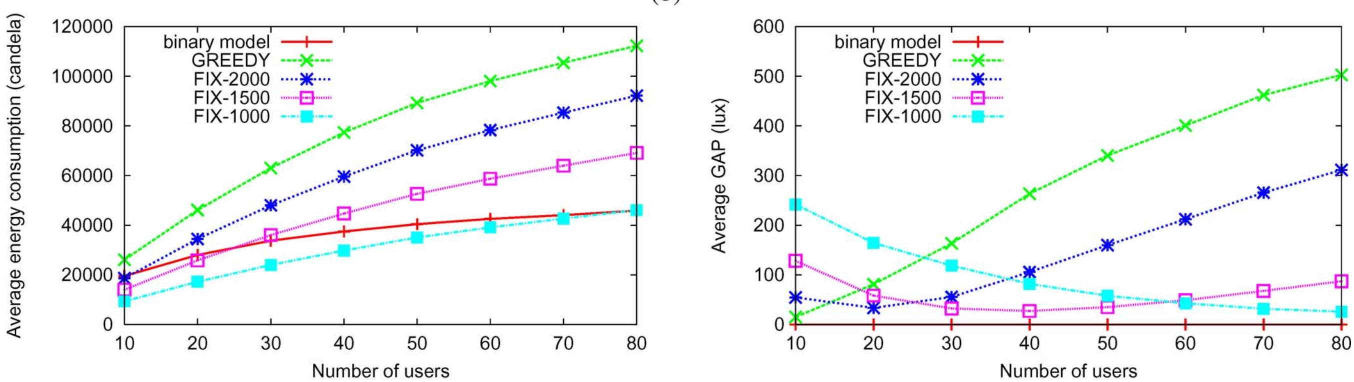

(c)

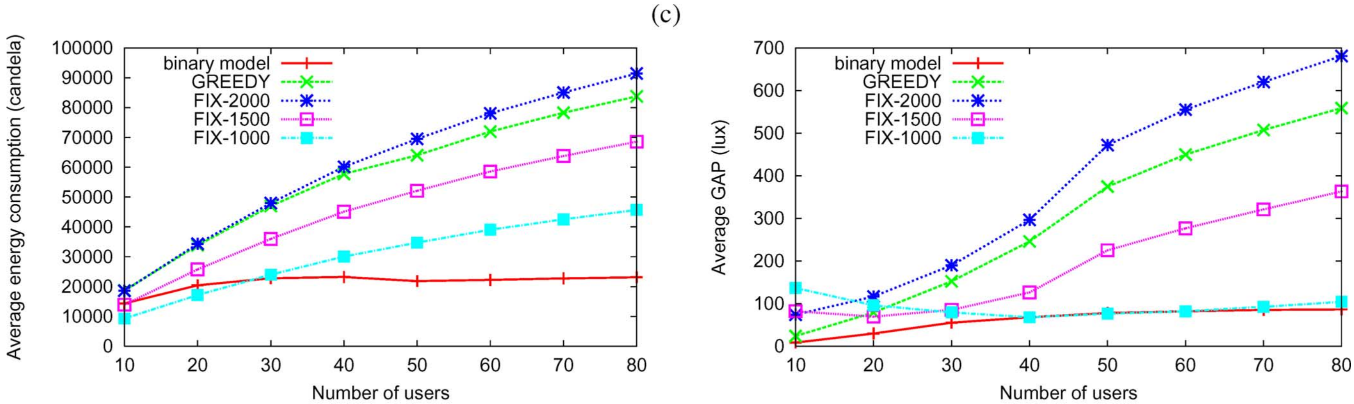

(d)

Fig. 11. Comparison under the binary satisfaction model: (a) network scenario $S1$ and pool $RP1$, (b) network scenario $S1$ and pool $RP2$, (c) network scenario $S2$ and pool $RP1$, and (d) network scenario $S2$ and pool $RP2$.

much larger. Fig. 11(b) adopts $RP2$. Because some requirements are violated, our scheme also induces some GAP. However, our scheme is also the most energy-efficient. Fig. 11(c) and (d) are the case of $S2$ and the trends are similar. This demonstrates that our scheme is quite scalable to network size.

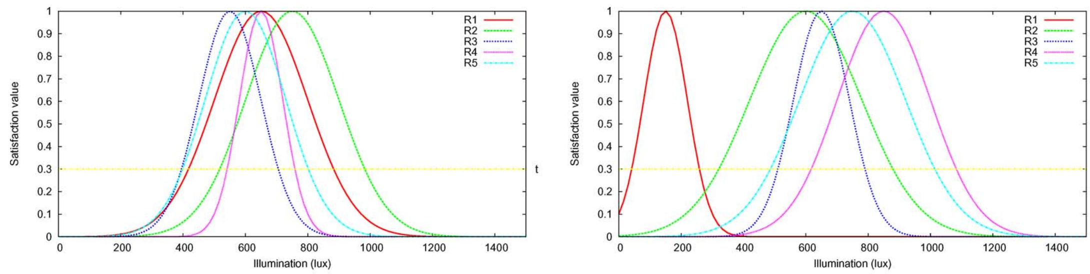

(a) (b)

Fig. 12. Requirement pools: (a) $RP3$ and (b) $RP4$.

- Continuous satisfaction model: We define two requirement pools $RP3$ and $RP4$, as shown in Fig. 12. Note that $RP4$ has higher deviation in requirements than $RP3$. The satisfaction threshold t is set to 0.3. We compare two performance indices: average user satisfaction and energy consumption. Fig. 13 shows our simulation results under different combinations of $S1/S2$ and $RP3/RP4$. These results consistently indicate that our scheme provides the highest satisfaction levels and outperforms FIX and GREEDY schemes in energy consumption.

VI. Prototyping Results

We have developed a prototype to verify our designs. Fig. 14 shows the system architecture. Users carry a badge with a built-in light sensor. The user's preference can be configured via the badge. The control host can make decisions and send them to lighting devices. We test our system in a room of size $8 \times 6\ \mathrm{m}^2$ with whole lighting devices deployed in a grid manner. Some demo videos of our work can be found at http://hscc.cs.nctu.edu.tw/iLight/. Below, we introduce each device, and then give our testing results.

A. User Badge and Light Sensor

The user badge has a wireless module Jennic (JN5139) [18], a light sensor (TSL230) [19], a TFT LCD panel (ILI9221) [20], and some input buttons. JN5139 is a single-chip microprocessor with an IEEE 802.15.4 [21] module. Fig. 15(a) illustrates the front and back views of the user badge. The outlook of a badge is like a bookmark. Users can specify their preferences via our graphic user interface (GUI) and buttons.

B. Whole Lighting Device

We use LEDs as light sources and deploy them on the ceiling. As shown in Fig. 15(b), each whole lighting device has a 4×4 LED module and a thermal pad is attached on its back for heat dissipation. We adopt pulse width modulation of digital input/output (DIO) to control the luminous intensity of light sources. Each LED has 20 levels of illumination, ranging from 0% to 100% luminous intensity. Fig. 15(c) shows our prototype.

C. iLamp

Fig. 15(d) shows the iLamp, which is composed of a robot arm, four sets of LEDs, and a JN5139 module. The robot arm consists of six Dynamical AX-12 actuators [22] as the lamp holder. Each AX-12 actuator can rotate from 0° to 300° at an accuracy of 0.33°. LEDs are similar to those used in whole lighting devices and with 20 levels of illuminations.

D. Control Host

Implemented by JAVA, the control host is the core of our system. It is composed of three components, including the *User Status Tracker*, *Decision Handler*, and *Device Controller*. By applying Java thread programming techniques, tasks are handled concurrently.

- User Status Tracker: This component checks current illuminations of all users periodically and, when needed, updates users' requirements. If it finds that a user's requirement is not satisfied or is updated, the Decision Handler will be triggered.
- Decision Handler: This component realizes our control algorithms. It is triggered by the User Status Tracker. The linear and nonlinear programming are resolved by the MATLAB Builder for Java [23]. The results are sent to the Device Controller to adjust lighting devices
- Device Controller: This is the interface between the control host and actuators. Commands are sent via RS232.

E. Performance Verification

We first verify the correctness of (1) through some tests. In Fig. 16(a), we fix h and ΔC_j^X and vary l from 30 to 230 cm. We measure the received illumination $\Delta L_{i,j}$ (in dash lines) and derive the ideal illumination (in solid line). The distance error between ideal and real values are calculated (in bars). As can be seen, the distance error is bounded by 10 cm. In Fig. 16(b), we fix h and l and vary ΔC_j^X from 40 to 400. We measure $\Delta L_{i,j}$ and calculate the distance error. Again, the gaps between the real distance and the derived distance are quite small.

Next, we verify our results in a real environment. We place 20 whole lighting devices in a $8 \times 6\ \mathrm{m}^2$ room in a grid-like manner. We adopt the same performance indices introduced in Section V. In Fig. 17, we compare the simulation and implementation results where there are 1 to 5 users. Each user may randomly select a requirement from requirement pools $RP1$ and $RP2$ for the binary satisfaction model or $RP3$ and $RP4$ for continuous satisfaction model. In all performance indices (average energy consumption, GAP, and satisfaction), the difference between simulation and implementation results are very close. The results indicate the correctness of our approaches. We further validate our results under different weather conditions, which may reflect to different nature light scenarios. Fig. 18

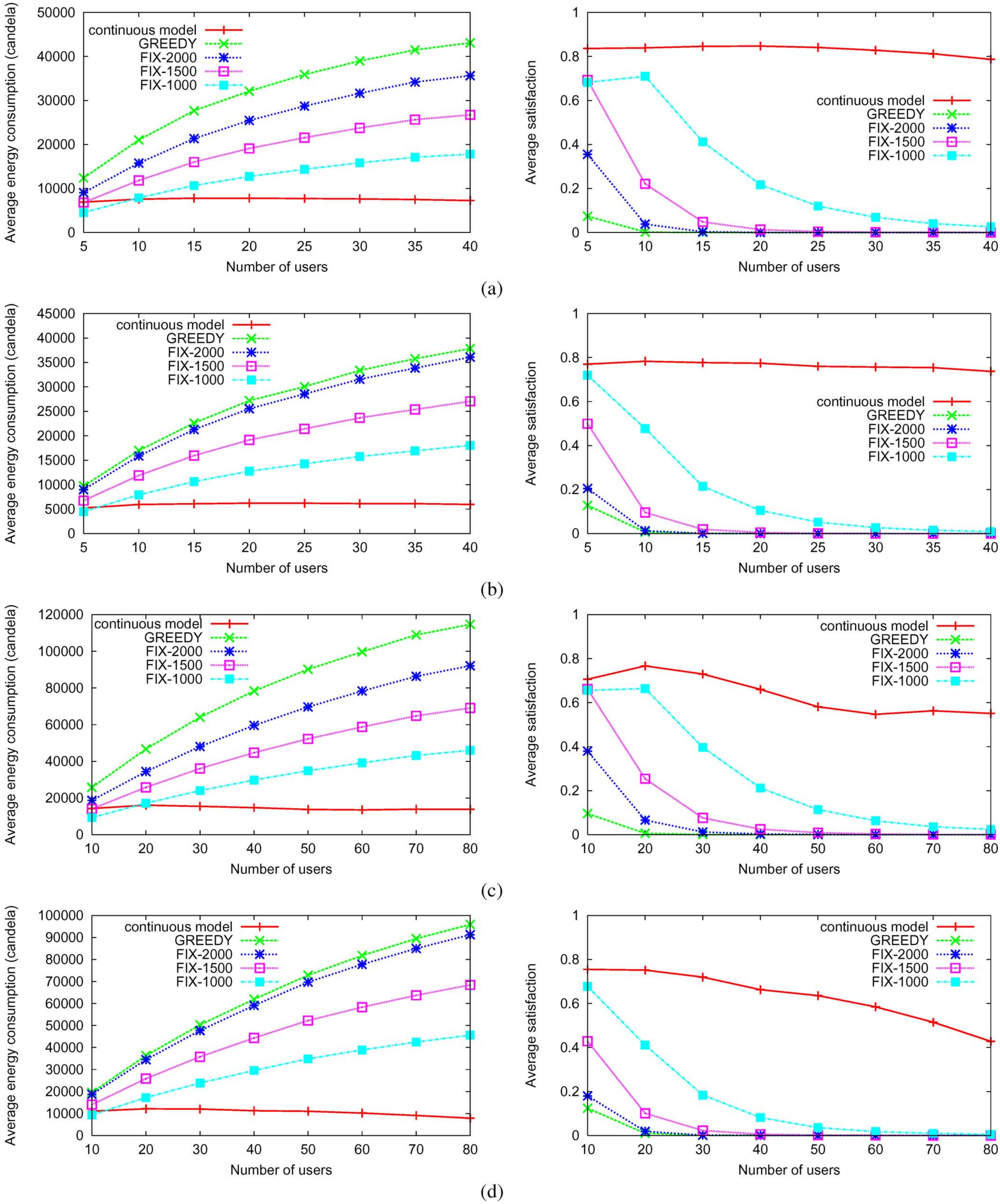

Fig. 13. Comparison under the continuous satisfaction model: (a) network scenario $S1$ and pool $RP3$; (b) network scenario $S1$ and pool $RP4$; (c) network scenario $S2$ and pool $RP3$; and (d) network scenario $S2$ and pool $RP4$.

shows the results by using the measured natural light as the index. We fix the number of users to three and randomly select their lighting requirements. There still exists high consistency between simulation and implementation results in most cases. Also, when the average natural light increases, the gap in energy consumption tends to become smaller.

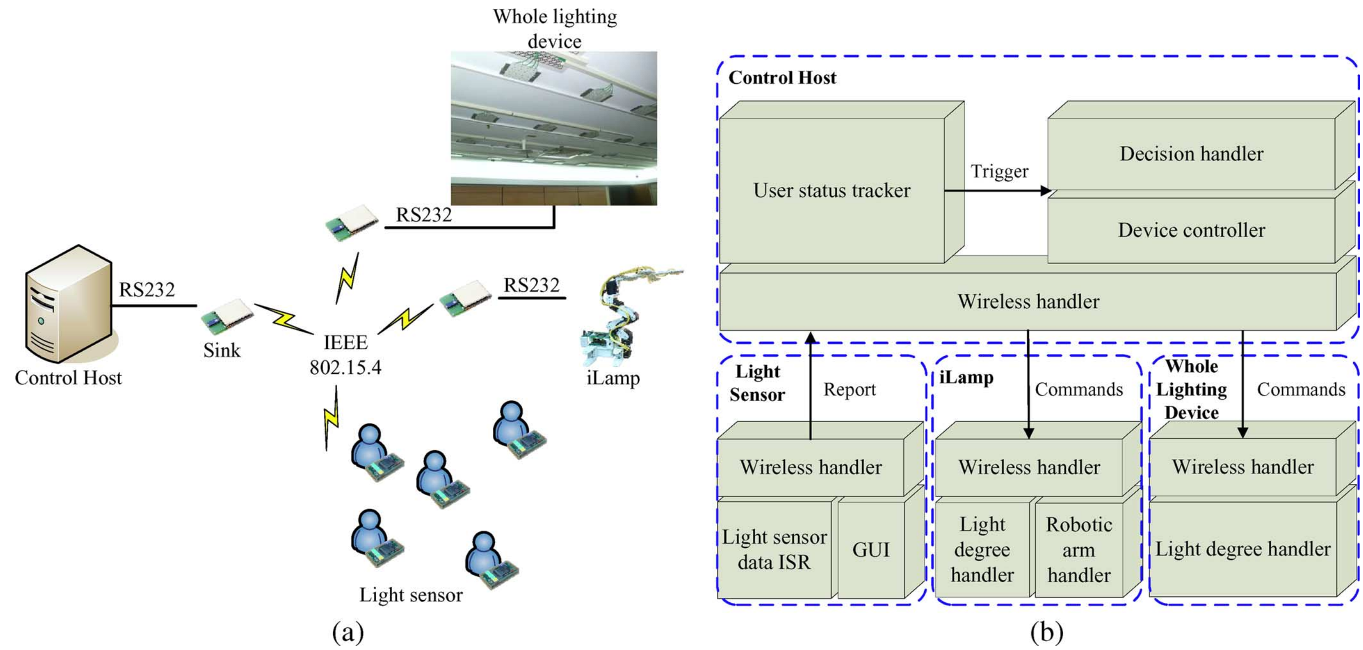

Fig. 14. Hardware and software system architecture of our prototype.

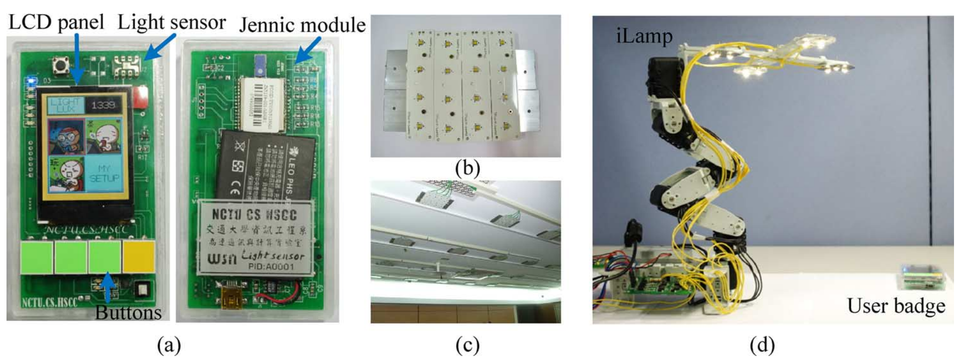

Fig. 15. (a) Front and back views of user badge, which looks like a bookmark; (b) whole lighting device; (c) testing environment; and (d) iLamp.

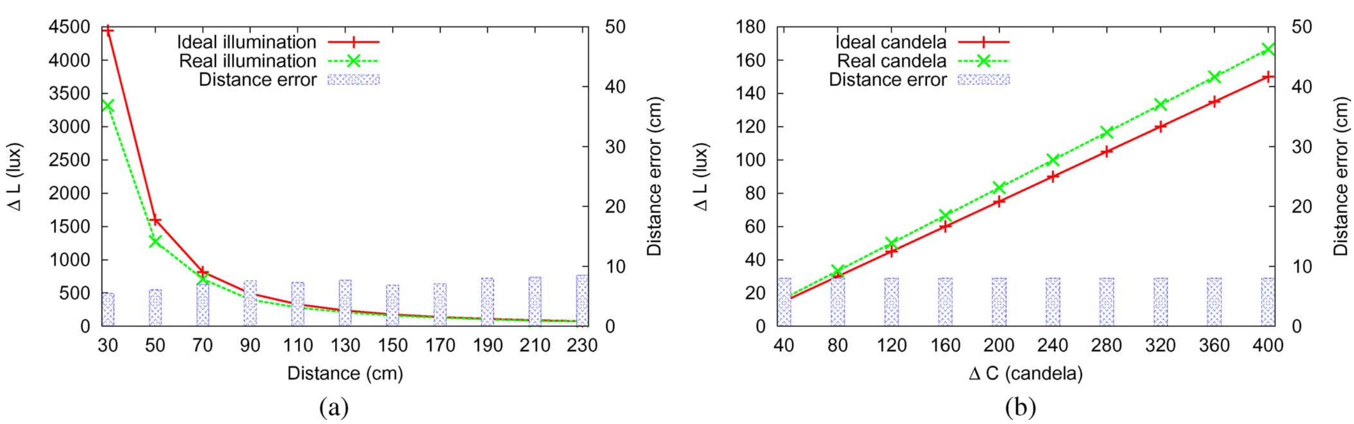

Fig. 16. Verification of (1): (a) fixing h and ΔC_j^X and varying l and (b) fixing h and l and varying ΔC_j^X.

For iLamp, we place a book on the desk and attach the light sensor on the book. We try to move the book (i.e, move the light sensor) from time to time. In this experiments, the ΔC is set to 12.25 candela. The average time for executing the algorithm of iLamp are about 3 seconds. (Steps 1 and 2 take about 1 second, and steps 3 and 4 take about 2 seconds.) This experiment shows that the amount of error of the angle pointing toward the light sensor is less than 15°.

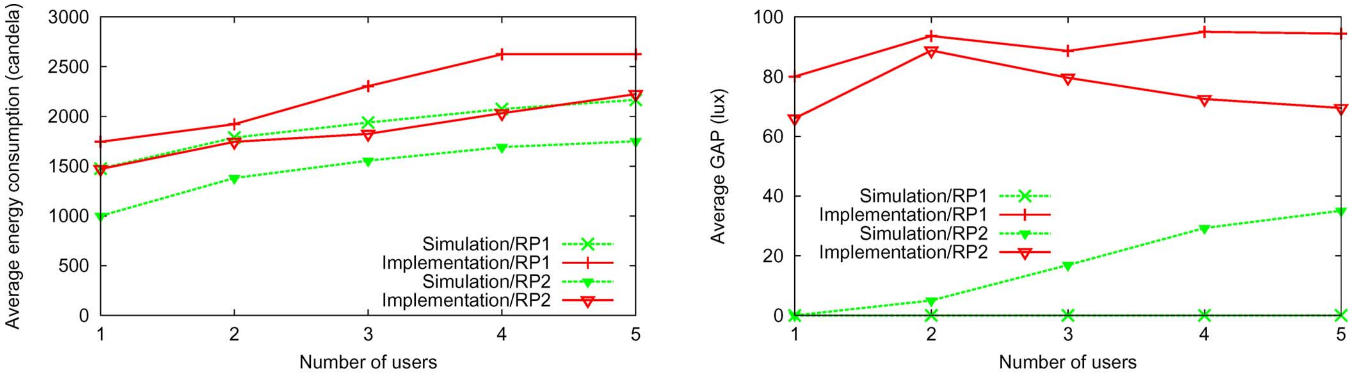

(a)

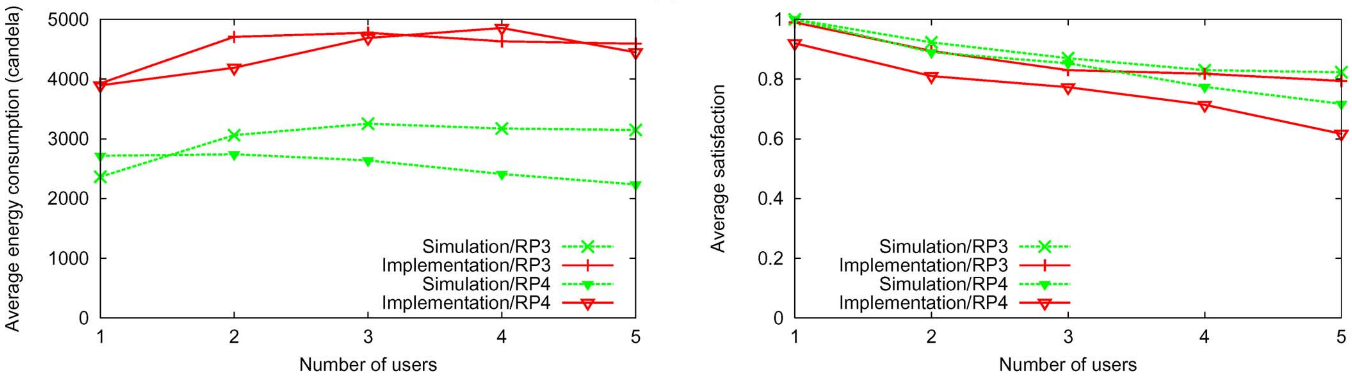

(b)

Fig. 17. Comparison of simulation and real implementation results under different numbers of users: (a) binary satisfaction model and pool $RP1$ or $RP2$, and (b) continuous satisfaction model and pool $RP3$ or $RP4$.

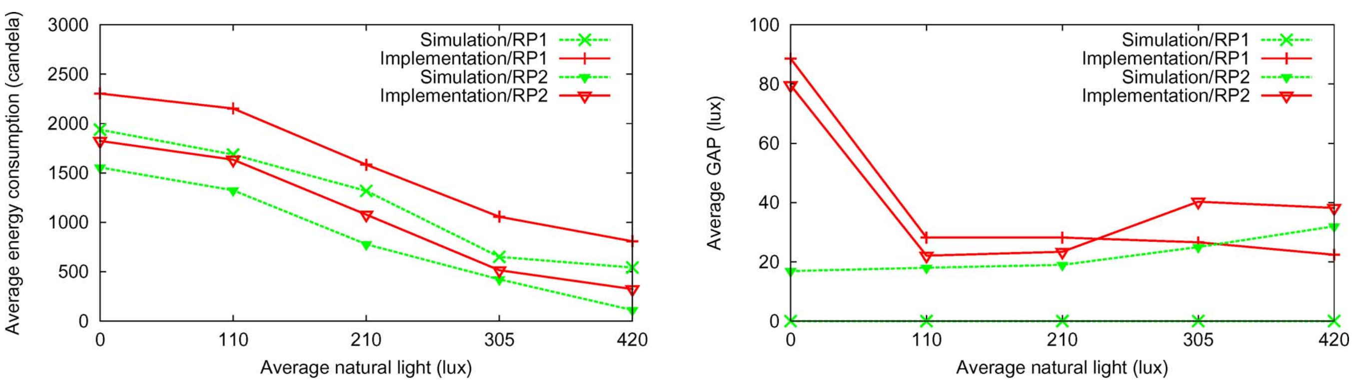

(a)

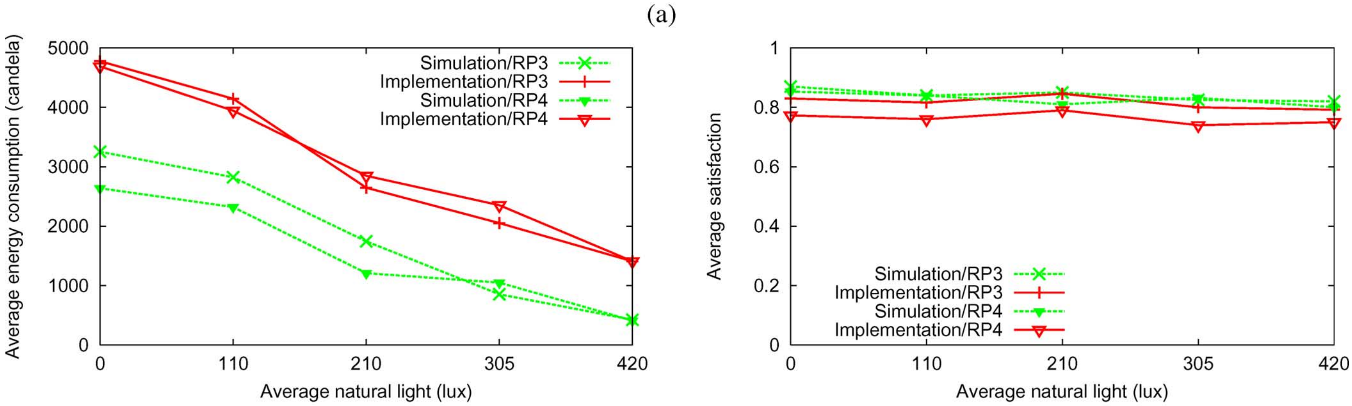

(b)

Fig. 18. Comparison of simulation and real implementation results under different natural light: (a) binary satisfaction model and pool $RP1$ or $RP2$ and (b) continuous satisfaction model and pool $RP3$ or $RP4$.

VII. Conclusion

We have presented an autonomous light control system. Both whole and local lighting devices are considered. For controlling whole lighting devices, two decision algorithms are proposed. For controlling local lighting devices, a novel surface-tracking scheme is proposed. Our system can dynamically adapt to environment changes and improve our earlier works by eliminating the requirement of tracking users' current locations. We evaluate our algorithms by simulations under different configurations. Besides, we have developed prototypes and deployed the whole system in a room to verify its effectiveness under real conditions. The results do show high consistency.

There is a basic limitation in our system. We enforce that users must carry light sensors to measure their current light intensities. This is due to the nature of light propagation. Without these light sensors, our system cannot get any information nearby the users. There are some alternatives, such as using motion sensors or thermal sensors to detect users' locations or rough light environments, respectively. Unfortunately, such approaches still cannot provide satisfactory solutions so far.

In Section III-B, we adopt Gaussian functions to represent users' satisfaction levels. However, the utility to human, in terms of light intensity, is still an unknown factor. This may deserve further study in the medical science field.

References

[1] H.-W. Gellersen, A. Schmidt, and M. Beigl, "Multi-sensor context-awareness in mobile devices and smart artifacts," *ACM/Kluwer Mobile Networks and Applications*, vol. 7, no. 5, pp. 341–351, 2002.

[2] M. Haenggi, "Mobile sensor-actuator networks: Opportunities and challenges," in *Proc. IEEE Int. Workshop on Cellular Neural Networks and their Applications*, 2002, pp. 283–290.

[3] Y.-C. Tseng, Y.-C. Wang, K.-Y. Cheng, and Y.-Y. Hsieh, "iMouse: An integrated mobile surveillance and wireless sensor system," *IEEE Computer*, vol. 40, no. 6, pp. 60–66, 2007.

[4] X. Wang, J. S. Dong, C. Chin, S. Hettiarachchi, and D. Zhang, "Semantic space: An infrastructure for smart spaces," *IEEE Pervasive Computing*, vol. 3, no. 3, pp. 32–39, 2004.

[5] S.-P. Kuo and Y.-C. Tseng, "A scrambling method for fingerprint positioning based on temporal diversity and spatial dependency," *IEEE Trans. Knowledge Data Eng.*, vol. 20, no. 5, pp. 678–684, 2008.

[6] D. Niculescu and B. Nath, "Ad hoc positioning system (APS) using AOA," in *Proc. IEEE INFOCOM*, 2003, pp. 1734–1743.

[7] A. Mainwaring, D. Culler, J. Polastre, R. Szewczyk, and J. Anderson, "Wireless sensor networks for habitat monitoring," in *Proc. ACM Int. Workshop on Wireless Sensor Networks and Appl. (WSNA)*, 2002, pp. 88–97.

[8] G. Werner-Allen, J. Johnson, M. Ruiz, J. Lees, and M. Welsh, "Monitoring volcanic eruptions with a wireless sensor network," in *Proc. Eur. Workshop on Sensor Networks (EWSN)*, 2005, pp. 108–120.

[9] M.-S. Pan, L.-W. Yeh, Y.-A. Chen, Y.-H. Lin, and Y.-C. Tseng, "A WSN-based intelligent light control system considering user activities and profiles," *IEEE Sensors J.*, vol. 8, pp. 1710–1721, 2008.

[10] H. Park, M. B. Srivastava, and J. Burke, "Design and implementation of a wireless sensor network for intelligent light control," in *Proc. Int. Symp. Inf. Process. Sensor Networks (IPSN)*, 2007, pp. 370–379.

[11] V. Singhvi, A. Krause, C. Guestrin, J. H. Garrett, and H. S. Matthews, "Intelligent light control using sensor networks," in *Proc. ACM Int. Conf. Embedded Networked Sensor Syst. (SenSys)*, 2005, pp. 218–229.

[12] Y.-J. Wen, J. Granderson, and A. M. Agogino, "Towards embedded wireless-networked intelligent daylighting systems for commercial buildings," in *Proc. IEEE Int. Conf. Sensor Networks, Ubiquitous, and Trustworthy Computing*, 2006.

[13] LED Lamp. [Online]. Available: http://en.wikipedia.org/wiki/LED_lamp

[14] *Light-Emitting Diode (LED)*. [Online]. Available: http://en.wikipedia.org/wiki/LED

[15] T. H. Cormen, C. E. Leiserson, and R. L. Rivest, *Introduction to Algorithms*. Cambridge, MA: MIT Press, 2001.

[16] J. Sankaran, "A note on resolving infeasibility in linear programs by constraint relaxation," *Oper. Res. Lett.*, vol. 13, no. 1, pp. 19–20, 1993.

[17] P. T. Boggs and J. W. Tolle, "Sequential quadratic programming," *Acta Numerica*, vol. 45, no. 1, pp. 1–51, 1995.

[18] *Jennic, JN5139*. [Online]. Available: http://www.jennic.com/

[19] *Light Sensor, TSL230*. [Online]. Available: http://www.taosinc.com/

[20] TFT LCD, ILI9221. [Online]. Available: http://www.ilitek.com/products.asp

[21] IEEE Standard for Information Technology – Telecommunications and Information Exchange Between Systems – Local and Metropolitan Area Networks Specific Requirements Part 15.4: Wireless Medium Access Control (MAC) and Physical Layer (PHY) Specifications for Low-Rate Wireless Personal Area Networks (LR-WPANs) 2003.

[22] *AX-12, Dynamixel Series Robot Actuator*. [Online]. Available: http://www.crustcrawler.com/motors/AX12/index.php

[23] *Matlab Builder for Java*. [Online]. Available: http://www.mathworks.com/products/javabuilder/

Lun-Wu Yeh received the B.S. and M.S. degrees in computer and information science from the National Chiao-Tung University, Hsin-Chu City, Taiwan, in 2003 and 2005, respectively. He is currently working towards the Ph.D. degree at the Department of Computer Science, National Chiao-Tung University.

His research interests include smart living space and wireless sensor network.

Che-Yen Lu received the B.S. and M.S. degrees in computer and information science and computer science from the National Chiao-Tung University, Hsin-Chu City, Taiwan, in 2007 and 2009, respectively.

His research interests include wireless sensor network and wireless communication.

Chi-Wai Kou received the B.S. degree from the National Tsing-Hua University, Hsinchu, Taiwan, in 2008. He is currently working towards the M.S. degree at the Department of Computer Science, National Chiao-Tung University, Hsin-Chu City, Taiwan.

His research interests include wireless communication and sensor networks.

Yu-Chee Tseng (SM'03) received the B.S. and M.S. degrees in computer science from the National Taiwan University and the National Tsing-Hua University, Hsinchu, Taiwan, in 1985 and 1987, respectively, and the Ph.D. degree in computer and information science from the Ohio State University Columbus, in January 1994.

He was an Associate Professor at the Chung-Hua University (1994–1996) and at the National Central University (1996–1999), and a Professor at the National Central University (1999–2000). Currently, he is Chairman of the Department of Computer Science, and Associate Dean of the College of Computer Science, National Chiao-Tung University, Taiwan.

Dr. Tseng is a member of ACM. He received the Outstanding Research Award by the National Science Council, R.O.C., in both 2001–2002 and 2003–2005, the Best Paper Award by the International Conference on Parallel Processing in 2003, the Elite I. T. Award in 2004, and the Distinguished Alumnus Award by the Ohio State University in 2005. His research interests include mobile computing, wireless communication, network security, and parallel and distributed computing.

Chih-Wei Yi (M'04) received the B.S. and M.S. degrees from the National Taiwan University, Taipei, in 1991 and 1993, respectively, and the Ph.D. degree from the Illinois Institute of Technology, Chicago, in 2005.

He is currently an Associate Professor of Computer Science at the National Chiao-Tung University. He was a Senior Research Fellow of the Department of Computer Science, City University of Hong Kong. His research focuses on wireless ad hoc and sensor networks, vehicular ad hoc networks, network coding, and algorithm design and analysis.

Prof. Yi is a member of ACM. He received the Outstanding Young Engineer Award from the Chinese Institute of Engineers in 2009.